

Application of Sentinel-2A Images for Land Cover Classification Using NDVI in Jember Regency

Rufiani Nadzirah* , Mochammad Kevin Rizqon, Indarto 

Department of Agricultural Engineering, University of Jember, Jember, 68121, Indonesia

*Corresponding author, email : rufianinadzirah@unej.ac.id

ARTICLE INFO

Received :
28 December 2021

Revised :
15 March 2024

Accepted :
26 March 2024

Published :
7 April 2024

ABSTRACT

The advancement of remote sensing technology has led to the development of sophisticated image processing methods that yield highly accurate land cover classification information, minimizing misinterpretations. The Normalized Difference Vegetation Index (NDVI) is a widely utilized method in remote sensing for measuring green vegetation. A significant portion of the Jember Regency area is covered by vegetation. This study aimed to identify various land cover types in the Jember Regency area, quantify the area for each classification, and establish the NDVI value ranges for each type of cover. Sentinel-2 was employed as the primary data source, and the NDVI method was utilized for land cover classification in the Jember Regency. The region exhibited diverse land cover types. Data from Sentinel-2A captured in June and October 2019 were chosen due to their accessibility, open-source nature, and adequate spectral, spatial, and temporal resolution. The classification in this study encompassed five classes: water bodies, settlements, dry fields, irrigated paddy fields, and forests. Error analysis was conducted using a confusion matrix with the Overall and Kappa algorithms. The accuracy results for June indicated a Kappa Accuracy of 37.7% and Overall Accuracy of 54.5%. In October, the Kappa Accuracy increased to 39.9%, and the Overall Accuracy reached 56.5%. In conclusion, the NDVI method did not meet the criteria for accurately interpreting land cover classification.

Keywords : Remote Sensing; NDVI; Sentinel-2A; Land Cover

INTRODUCTION

The use of remote sensing for monitoring land conditions has proven to be a highly effective and efficient approach, requiring less time (da Silva et al., 2020; Dronova, 2015), as demonstrated by Tao et al. (2019). High-resolution satellite images offer a powerful tool for analyzing various features on the Earth's surface (Ahmed & Singh, 2020). They enable the identification of land cover in specific regions (Adam et al., 2010; Indarto, 2014; Putra et al., 2019; Zhang et al., 2019) and enhance the precision of estimating crop planting areas (Sun et al., 2019). Specifically, Sentinel-2A imagery, provided by the European Space Agency (ESA), with its spatial resolution of 10 meters, proves valuable for analyzing diverse land cover types, especially in heterogeneous areas (Osgouei et al., 2019; Preidl et al., 2020; Saini & Ghosh, 2019). However, it's important to acknowledge that visual image analysis does have its limitations, particularly in situations involving cloud cover and shadow, as noted by Preidl et al. (2020). The accuracy of visually interpreting an image is heavily influenced by the object being interpreted and the image's resolution quality (Andiko et al., 2019).

Jember is a regency situated in the eastern part of the East Java Province, covering an area of 3,293.44 km². The area consists of 31 districts and 248 sub-districts. This regency has a varied land cover, and most of the green regions comprised forests, paddy fields, fields, and plantations (Badan Pusat Statistik, 2019). It is essential to monitor land use maintenance to help observe and analyze natural resources so that the sustainability of natural resources can be sustained (Patel et al., 2019; Vali et al., 2020; Zhao et al., 2019).

In this study, an analysis of land cover in Jember Regency was conducted using Sentinel-2A image data from 2019 as the raw data. The study employed the Normalized Difference Vegetation Index (NDVI) method, a commonly used technique for comparing vegetation greenness in satellite image data (Kawamuna et al., 2017). NDVI serves as an indicator for biomass conditions, representing the level of greenness in vegetation based on chlorophyll values and aiding in the assessment of vegetation health status (Velooso et al., 2017). Additionally, NDVI enhances graphic visualization (Goncalves et al., 2019) and normalizes the effects of lighting changes, surface slope, and aspect (Sotille et al., 2020). Given that a predominant portion of land cover in the Jember Region is vegetation, the NDVI method was chosen accordingly to evaluate NDVI values. The objective of this study was to assess various land cover types and analyze the accuracy of land cover classification results in Jember Regency using the NDVI method.

METHODS

Study Area

Jember is a regency situated in the eastern part of East Java Province, covering an area of 3,293.44 km². It is subdivided into 31 districts and 248 sub-districts. Geographically, Jember Regency is positioned between 113°15'47" to 114°02'35" E longitude and between 7°58'06" to 8°33'44" S latitude. The regency shares its boundaries; to the north, it adjoins Probolinggo Regency and Bondowoso Regency, to the east it borders Banyuwangi Regency, to the south it meets the Hindia Ocean, and to the west it is adjacent to Lumajang Regency. The dry season typically spans from May to October, while the rainy season occurs from November to April. The relative humidity in this region is recorded at 74.25%, with an average temperature of 28.2°C. This research encompasses the entire area of Jember Regency, including all 31 districts (Figure 1). The study was conducted from February to June 2020 (Badan Pusat Statistik, 2019).

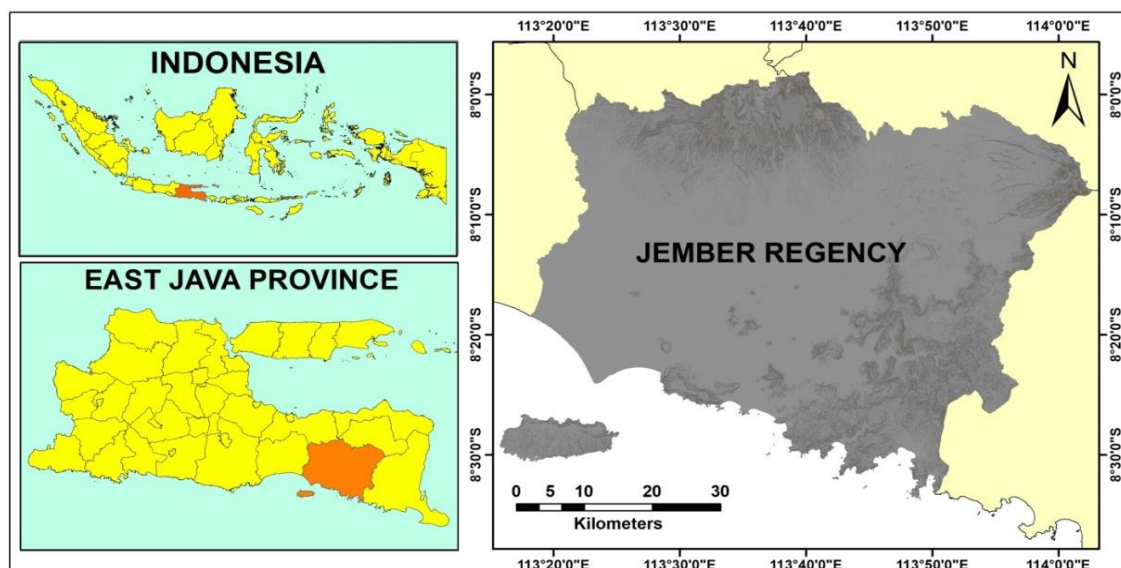


Figure 1. Study Area

Material

The tools used in this research were the Global Positioning System (GPS), open-source software QGIS 3.10.2, and a smartphone camera. The materials used in this study were Sentinel-2A satellite images data (Table 1) for June and October 2019, district boundaries, and Ground Control Point (GCP). The procedure of this study was an inventory of Sentinel-2A images data in June and October 2019. Sentinel-2A images were obtained from the United States Geological Survey (USGS). Then pre-processing was preparing the raw data before it was processed by modifying detailed images (Pandey et al., 2017). Pre-processing in this study consisted of atmospheric correction, mosaicking of four Sentinel-2a images and clipping images according to the boundaries of the Jember Regency. In addition, other than images data, the raw data needed was field survey data used as GCP. After that, the data was processed in three processes, namely NDVI transformation, NDVI identification, and image classification. After the data had been processed, the Overall and Kappa Accuracy tests were tested in both classification results data in June and October 2019.

Table 1. Sentinel-2A Images List

ID	Acquisition Date	Platform	Tile Number
L1C_T49LGL_A020921_20190625T024403	June 25, 2019	S-2A	T49LGL
L1C_T49MHM_A020921_20190625T024403	June 25, 2019	S-2A	T49MHM
L1C_T49LHL_A020921_20190625T024403	June 25, 2019	S-2A	T49LHL
L1C_T49MGM_A020921_20190625T024403	June 25, 2019	S-2A	T49MGM
L1C_T49LGL_A022637_20191023T023735	October 23, 2019	S-2A	T49LGL
L1C_T49MHM_A022637_20191023T023735	October 23, 2019	S-2A	T49MHM
L1C_T49LHL_A022637_20191023T023735	October 23, 2019	S-2A	T49LHL
L1C_T49MGM_A022637_20191023T023735	October 23, 2019	S-2A	T49MGM

Data Inventory

The data inventory process consisted of images downloaded and field surveyed for GCP. Sentinel-2A images downloaded from <https://earthexplorer.usgs.gov/> (USGS, 2019). The requirement for downloaded Sentinel-2A images data was only had cloud cover less than 10% in each scene so that the cloud cover does not interfere with the analysis process. GCP was taken from the field survey results by creating a control point using GPS. Figure 2 shows 557 points containing information about the types of land cover in the Jember Regency were obtained.

Pre Processing

The pre-processing step consisted of atmospheric correction and image cropping. The atmospheric correction process used the Dark Object Subtraction (DOS) method available on the Semi-Automatic Classification Plugin (SCP) from the QGIS software (Cui et al., 2014; Firmansyah et al., 2019). . DOS is a method to improve radiometric values in images due to atmospheric disturbances. DOS has an approach that dark-colored objects or usually water, dense forests, and cloud shadows should have a 0 value pixel. If the thing is not worth 0, that value was biased (Kristianingsih et al., 2016).

Furthermore, images clipping was carried out based on the boundaries of the study area, namely Jember Regency. Clipping was done using vector data of the Jember Regency boundaries. Vector data that was the Jember Regency boundary was downloaded from the <http://tanahair.indonesia.go.id/portal-web/> page (Badan Informasi Geospasial, 2017). The clipping process was carried out before data processing became smaller than before the clipping process, and the data processing process was not too heavy.

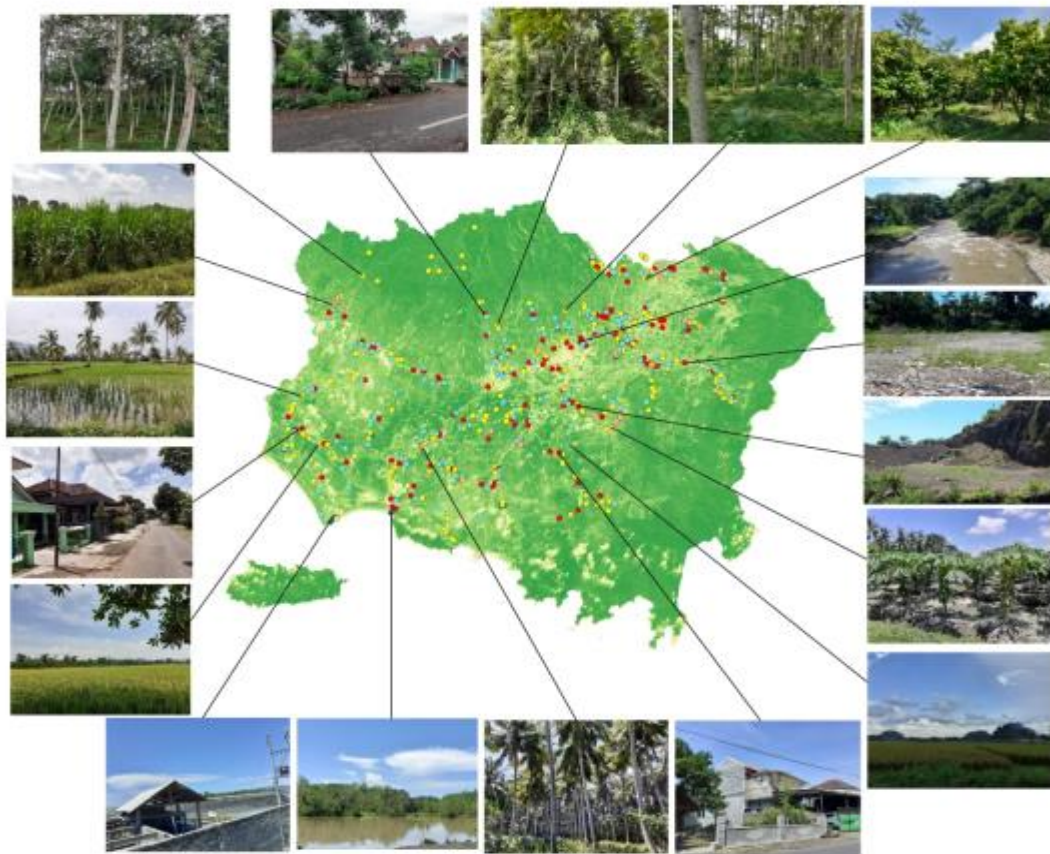


Figure 2. Ground Check Points (GCP) Location

Data Processing

The data processing stage consists of NDVI transformation, identification of NDVI values, and image classification. Sentinel-2A image transformation to NDVI using band $(NIR-RED)/(NIR+RED)$ algorithm. The NDVI transformation helps change the pixel values in the range of -1 to 1 so that NDVI can easily distinguish areas with chlorophyll from other land covers. Next, identify the spectral values to determine those contained in several GCPs as a reference for classification. In this process, validation in the field using GCPs. Spectral values were taken at the smallest pixels included in each GCPs, followed by a range of spectral values based on the known vegetation density in each predetermined class, namely water bodies, settlements, dry land, dry fields, paddy fields, plantation/forests. The last process was image classification to classify the pixel values in each class based on the range of NDVI spectral values that have been obtained (Putra et al., 2017).

Accuracy Test

The accuracy test of the classification was used to get the accuracy of a method on remote sensing. One of the standard methods used was the confusion matrix (Simamora et al., 2015). According to (LAPAN, 2014), the guideline for processing satellite data is that the classification accuracy assessment level must be no less than 75%. An example of a confusion matrix can be seen in Table 1. We used Overall and Kappa Accuracy to determine accuracy of classification (Clerici et al., 2017). Figure 3 shows research procedure which used from preparation, pre-processing, processing, and data analysis.

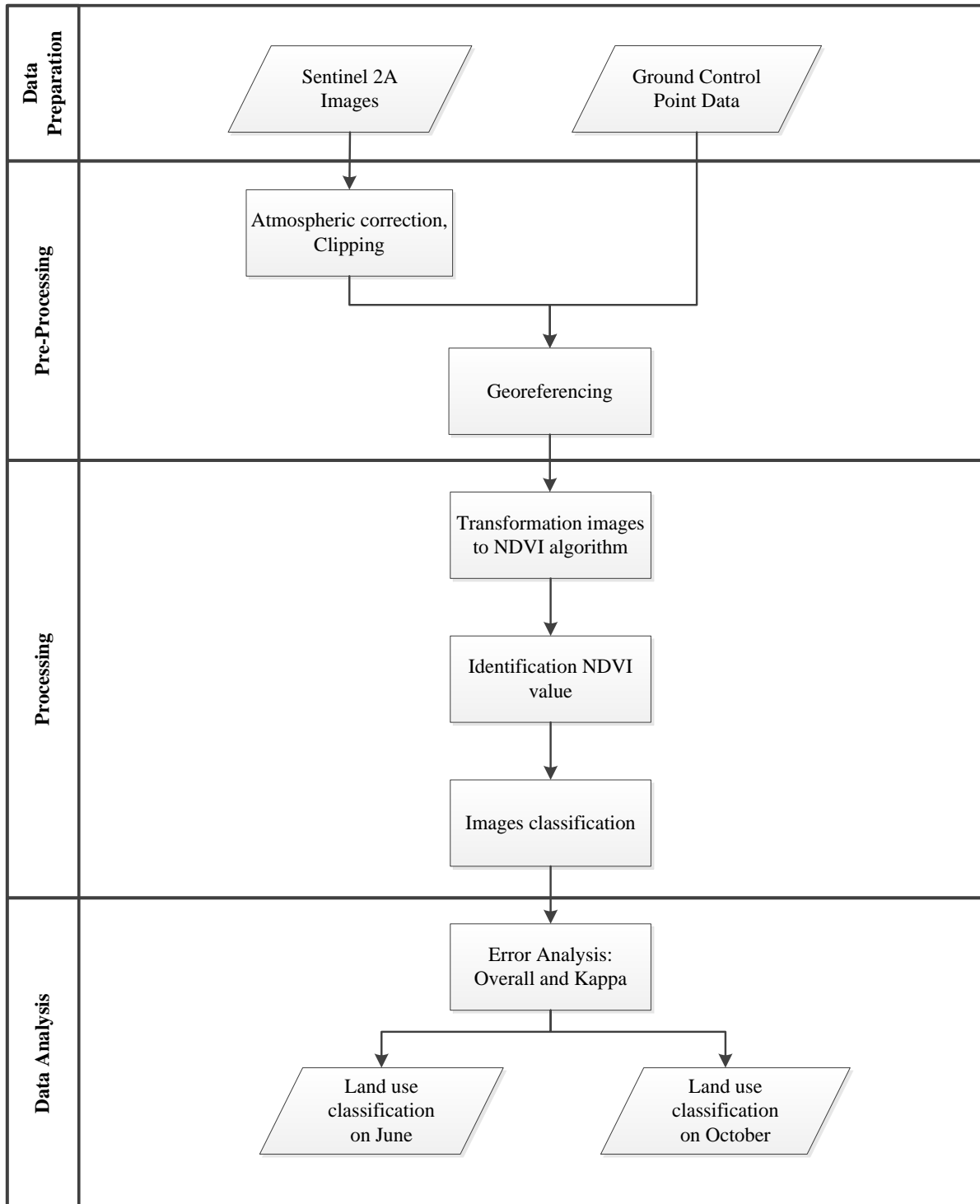


Figure 3. Research procedures

RESULTS AND DISCUSSION

Normalized Difference Vegetation Index

NDVI was used to see the vegetation density in the study area (Bontemps et al., 2015; Goncalves et al., 2019). Sentinel-2A image transformation to NDVI using $(\text{NIR-RED})/(\text{NIR+RED})$ algorithm (Sotille et al., 2020). The choice of capturing images in both June and October stems from the distinct seasons represented by these months, dry for June and rainy for October. Utilizing NDVI time series derived from these months allows for an accurate reflection of vegetation growth and provides valuable information for distinguishing vegetation types, especially concerning seasonal and phenological changes (Sun et al., 2019). Temporal analysis proves to be the most suitable approach for analyzing land cover change information, enabling consistent and repeatable measurements across various spatial scales. This approach is well-suited for capturing the processes of change occurring on the Earth's surface (Ahmed & Singh, 2020).

The NDVI results indicated that a greener color in the images corresponds to higher vegetation index values, while a redder color indicates a lower vegetation level. The NDVI value for any pixel falls within the range of minus one (-1) to plus one (+1) (Ahmed & Singh, 2020), and non-vegetated pixels yield values close to zero. Negative values typically indicate non-reflective surfaces such as clouds, snow, or water, while positive values suggest vegetated or reflective surfaces (Tao et al., 2019; Wong et al., 2019). The results of NDVI can be seen in Figure 4 below.

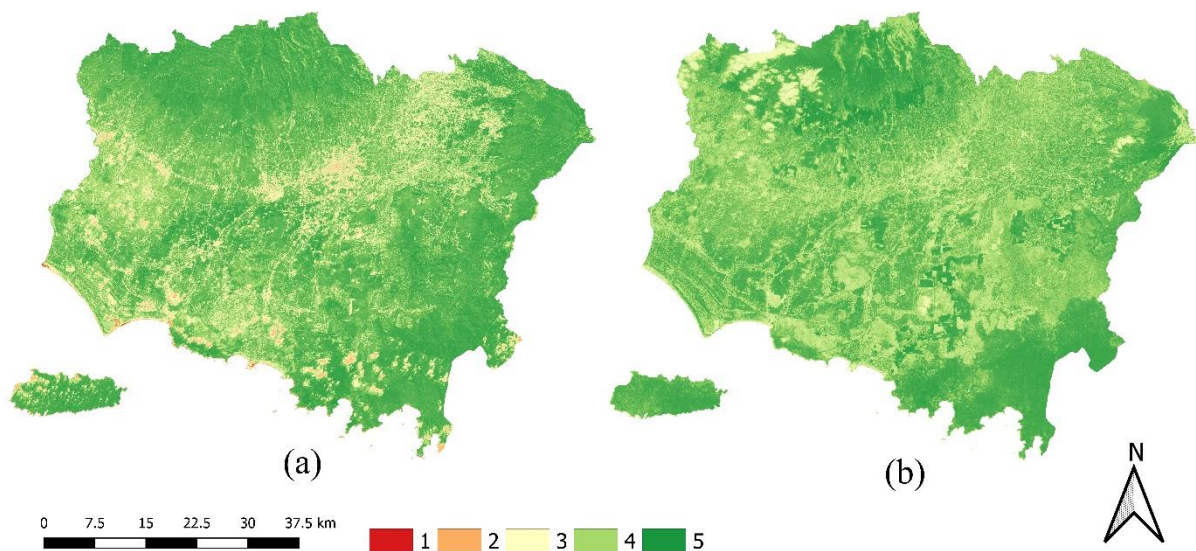


Figure 4. (a) NDVI in June, (b) NDVI in October
(1) -1 to -0.6; (2) -0.6 to -0.2; (3) -0.2 to 0.2; (4) 0.2 to 0.6 (5) 0.6 to 1

In the analysis, the northern and eastern areas were predominantly green, indicating forested or garden areas. Conversely, in the southern region, a considerable amount of reddish-yellow color was observed, indicative of built-up land or residential areas. However, the transformation results differed. For instance, in the northern region in June, the dominant color was green, whereas in October, yellow color prevailed due to cloud cover affecting the imagery.

The middle area also shows a different color. The color in June was reddish yellow, while in October, it is greenish-yellow. This research indicated that different seasons produce different NDVI. There are many fields in June or the dry season, while in October or the rainy season, the areas of the fields were turned into irrigated paddy fields. Da Silva et al (2020) verified in wheat phenology that temporal variations of the NDVI peak position due to climatic variations, and also

spatial changes in relation to latitude in the Northern China Plain as well. In this study, the area that had high NDVI value mostly was in highland area such as north-west, north-east, and south-east area. On the other hand, images quality also affects the NDVI results. According to (Arnanto, 2013), all images obtained through sensor recording have error values, one of the causes of which is the sensor recording mechanism, the motion and geometry of the earth, and atmospheric conditions at the time of recording.

Identification of Spectral Value

The spectral values of the NDVI transformation results that have been identified from each class can be seen in Table 2.

Table 2. NDVI values for each land cover class

Classification	Total GCPs	NDVI Value	
		June	October
Water Body	13	-0.125 – 0.627	0.005 – 0.722
Settlement	130	0.044 – 0.770	0.041 – 0.789
Field	32	0.187 – 0.852	0.250 – 0.720
Paddy Field	138	0.144 – 0.842	0.112 – 0.829
Plantation/Forest	244	0.299 – 0.861	0.053 – 0.918

Analyzing the data in Table 2 revealed distinct NDVI values for each land class. The data illustrated that denser vegetation, such as forests, had higher NDVI values, while non-vegetated areas like settlements and water bodies displayed lower values. This observation aligns with the information provided by the Minister of Forestry of the Republic of Indonesia (Menteri Kehutanan Republik Indonesia, 2012), who stated that NDVI values ranging from -1 to -0.03 signify unvegetated land, whereas land with a high vegetation level falls within the range of 0.36 to 1. The NDVI calculation, based on band ratios, is designed to normalize the influence of factors like lighting changes, surface slope, and aspect (Sotille et al., 2020). However, it's important to note that some spectral values experienced overlap with other classes. This overlap occurred because many NDVI results did not precisely match the field conditions. Additionally, the variety of vegetation types in the study area affected the NDVI values, as stated by Arnanto (2013) which stated that the effectiveness of digital image analysis using the vegetation index transformation method is more pronounced for identifying objects with broad and homogeneous distribution characteristics.

Determination of NDVI Value Range

The range of NDVI values is -1 to 1. The determination of the range of NDVI values was used as a reclass or as a classification reference. Table 3 below is an example of determining the range of NDVI values in one class.

Table 3. NDVI value of water body

Classification	GCPs	NDVI Value
Water Body	1	-0.125
	2	-0.102
	3	-0.006
	4	0.007
	5	0.019
	6	0.062
	7	0.087
	8	0.087
	9	0.180
	10	0.208
	11	0.288
	12	0,346
	13	0,627

Table 3 showed that the yellow color in the table was the mode of the NDVI value of the water body. This value was used as the maximum value for the water body class while the maximum value for the water body class was -1 because the NDVI value for the water body was the lowest, so it used the lowest NDVI value. The other classes minimum and maximum values were determined by using the previous class mode as the lower limit and the class mode identified as the upper limit. Below in Table 4 is the range of NDVI values for each class.

Table 4. Range of NDVI values for each classification class

Classification	Total GCP	NDVI Value	
		June	October
Water Body	13	-0.125 - 0.087	0.005 - 0.149
Settlement	130	0.088 - 0.334	0.150 - 0.317
Field	32	0.335 - 0.658	0.318 - 0.416
Paddy Field	138	0.659 - 0.740	0.417 - 0.680
Plantation/Forest	244	0.741 - 0.861	0.681 - 0.918

The table above shows the data for each class range of NDVI values. The NDVI values in June and October did not have the same degree because the two months were in different seasons. The content of NDVI values in June or the dry season tends to be lower than in October or the rainy season. This result was because, in the dry season, most of the vegetation loses its leaves. In contrast, the previously dry land becomes fertile in the rainy season and causes the foliage to become denser and denser. According to Arnato (2013), in the rainy season, the vegetation canopy cover is relatively thicker when compared to the canopy cover in the dry season, which affects the pixel value of the digital image.

Classification Result

The NDVI Sentinel-2A images classification produced five classes; water bodies, settlements, dry fields, paddy fields, and forests. The classification was based on a predetermined range of spectral values. The following in Figure 5 is a map of the results of the NDVI classification.

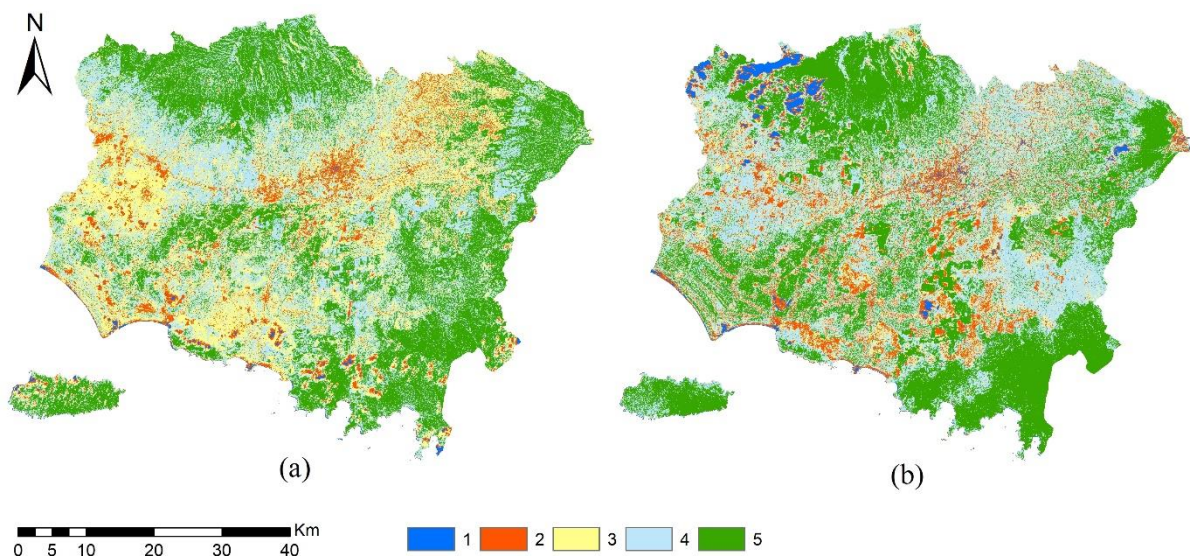


Figure 5. (a) Classification map in June; (b) Classification map in October. (1) water bodies and cloud cover, (2) settlements, (3) fields, (4) paddy fields, (5) plantation/forests.

Image classification to map land cover using the NDVI method is not new in remote sensing. However, there were still some errors in interpretation. Figure 3 above shows the NDVI classification resulting in five land cover classes. The five classes were water bodies, settlements, dry fields, paddy fields, and plantations/forests. Two classes could not be classified using NDVI, such as dry land and cloud cover. The dry land class in the NDVI classification results in one with the settlement because the characteristics of dry land and settlements were similar so that the resulting values were closed. In the residential area in question, the roof of the house in the form of tile with the primary soil material had the same value as dry land, which was also dominant with soil. In the cloud cover class, the results of the NDVI classification become one with a body of water. This result is because the cloud transformed with NDVI will darken so that the resulting value is the same as the water body class value.

Vegetation variability also dramatically affects the pixel value in the images. The type of vegetation in the Jember Regency was heterogeneous. The differences in leaf structure for each kind of vegetation greatly affected the NDVI value in the images. According to [Arnanto \(2013\)](#), the primary influence on the characteristics of leaf reflection among various plant species was the difference in leaf thickness which results in differences in pigment and leaf physiological structure. The following in [Figure 6](#) is an example of a comparison of the results of the classification, digital globe image, and the Indonesian Earth Map.

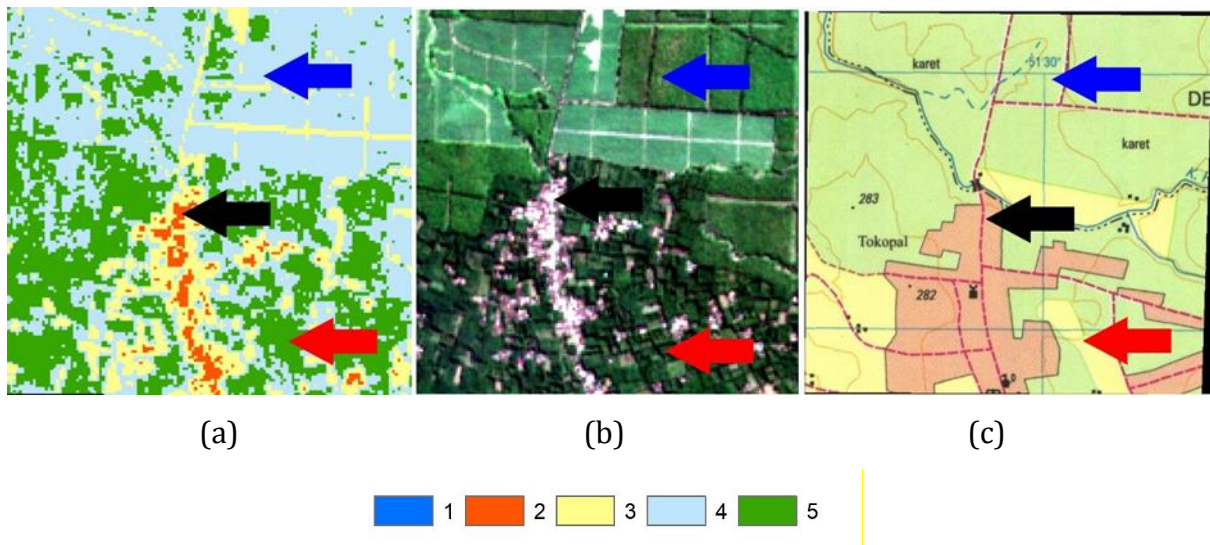


Figure 6. (a) classified image, (b) digital globe image, (c) the Indonesian Earth Map image
(1) water bodies and cloud cover, (2) settlements, (3) fields, (4) paddy fields,
(5) plantation/forests.

The images fragment in [Figure 6](#) was of the Silo District area. This comparison was used to determine the accuracy of the interpretation of the NDVI classification method based on digital globe images in 2019 and RBI maps in 2011. The black arrows on the NDVI classification image indicate residential areas represented in red. The digital globe image and RBI map also show the same site: settlements. The blue arrows in the NDVI classification image showed irrigated rice fields represented in light blue, while the digital globe imagery and RBI map showed plantations.

The difference in classification was because the irrigated paddy fields in the NDVI classification have a high range of values. The classification results were not following actual conditions because the plantation area was considered a paddy field. The red arrow in the classified image indicates the forest area. The digital globe image shows the same result: forest, but it offers a dry location on the RBI map. The difference was because the RBI map was published in 2011 by the Indonesian Geospatial Information Agency, so that land cover changes were most likely to occur.

Calculation of Classification Area

Calculation of land area in the NDVI method was done by multiplying the percentage of each polygon with the total area in the study area to determine the area of each class classified. The following in [Tables 5](#) and [6](#) are the results of the land area of each class from the NDVI classification.

Table 5. Classification Area in June

No.	Classification	Area (km ²)	Area (%)
1	Water Body	17.5	0.53
2	Settlement	212.24	6.41
3	Field	835.52	25.24
4	Paddy Field	1125.12	33.98
5	Plantation/Forest	1120.27	33.84
Total		3310.64	100

Table 6. Classification Area in October

No.	Classification	Area (km ²)	Area (%)
1	Water Body	61.54	1.86
2	Settlement	342.52	10.35
3	Field	340.22	10.28
4	Paddy Field	1320.11	39.87
5	Plantation/Forest	1246.25	37.64
Total		3310.64	3310.64

Based on the data in [Tables 5](#) and [6](#), the results of the land cover area in June were 17.5 km² of water bodies, 212.24 km² of settlements, 835.52 km² of fields, 1125.12 km² of paddy fields, and 1120.27 km² of forests. Meanwhile, there were 61 km² of water bodies in October, 342.53 km² of settlements, 340.23 km² of fields, 1320.12 km² of rice fields, and 1246.26 km² of forests. In October, the water body class experienced an increase in land area from June. In October, the rainy season had entered so that rivers that were not classified as water bodies in the dry season became rivers classified as water bodies. The rice field class also experienced increased land due to much dry land being converted into irrigated rice fields. In addition, the forest also experienced an increase in the land area because green lands such as dry fields and rice fields were seen brightly due to the thickening of the canopy cover, so that some were classified as forest. This is following the statement of [Arnanto \(2013\)](#) that the canopy cover of vegetation in the rainy season was likely relatively thicker than in the dry season. The difference in the thickness of the canopy cover will affect the pixel value of the digital image. Therefore, field monitoring should consider key parameter such as canopy cover ([Tsakmakis et al., 2021](#)).

Accuracy Test

The accuracy test was conducted using the confusion matrix or contingency matrix and then calculating with the overall and Kappa equations. Below in [Tables 7](#) and [8](#) are the accuracy calculations with the confusion matrix.

Table 7. Confusion matrix in June

Classification	Water Body	Settlement	Field	Paddy Field	Plantation/Forest	Total
Water Body	8	3	2	0	0	13
Settlement	1	98	28	2	1	130
Field	0	4	7	12	9	32
Paddy Field	0	26	43	39	30	138
Plantation/Forest	0	2	24	66	152	244
Total	9	133	104	119	192	557

Note : Overall accuracy = 54.5%
Kappa accuracy = 37.7%

Table 8. Confusion matrix in October

Classification	Water Body	Settlement	Field	Paddy Field	Plantation/Forest	Total
Water Body	8	3	0	1	1	13
Settlement	18	99	11	0	2	130
Field	0	6	11	13	2	32
Paddy Field	1	20	13	67	37	138
Plantation/Forest	3	10	7	94	130	244
Total	30	138	42	175	172	557

Note : Overall accuracy = 56.5%
Kappa accuracy = 39.9%

From the data in [Tables 7 and 8](#), the accuracy value had been calculated using the Kappa and Overall equations. The accuracy value obtained in June is Overall at 54.5% and Kappa at 37.7%. In October, the accuracy value acquired was Overall at 56.5% and Kappa at 39.9%. According to [LAPAN \(2014\)](#), results of accuracy test must be above 75%. Thus, the NDVI Sentinel-2A image classification results are not suitable for use because the accuracy rate is less than 75%.

Several factors that affect the low level of accuracy test include the green land cover class having the problem of overlapping NDVI values because the vegetation of the study area was a primarily heterogeneous forest. Many forest pixels are classified as rice fields and rice fields as forests. This result is because forests and rice fields have almost the same characteristics or similar spectral value ([Saini & Ghosh, 2019](#)). The resulting values are also nearly the same and even overlap and cause some information to be hidden and could not be appropriately interpreted ([Huang et al., 2017](#)). According to [Arnanto \(2013\)](#), heterogeneous vegetation areas make it difficult to extract information from the image so that the accuracy of the classification results is minimal. Digital image analysis with vegetation index was effective against homogeneous study objects. In addition, the image used was still a lot of cloud cover so that the area covered by cloud shadows produces a different class from the actual situation in the field ([Yang et al., 2019](#)), because cloud mask product was not reliable ([Zhang et al., 2018](#)) and observing earth surfaces should consider cloud cover ([Filgueiras et al., 2019; Preidl et al., 2020](#)).

[Zhang et al. \(2019\)](#) conducted a study in which they discovered that utilizing a specific band selected through the Mutual Information (MI) method resulted in higher accuracy compared to using all 13 bands of Sentinel-2. This approach also outperformed index-based and index-related methods such as NDVI and Normalized Difference Water Index (NDWI). The study by Zhang and colleague's sheds light on the lower accuracy observed in this current study. In this study, index-related bands, including those involved in NDVI that utilize data from the Near-Infrared bands and Red were employed. The MI method, mentioned by [Zhang et al. \(2019\)](#), is a feature scoring algorithm used for feature selection, assigning a score value to each feature to reflect its usefulness in classification problems.

Classification errors in this study have a reasonably high value. It was better to use a combination of NDVI and SAVI ([Vani & Mandla, 2017](#)) or EVI ([Vijith & Dodge-Wan, 2020](#)) for further research to increase the NDVI value so that images interpretation will make more accurate in heterogeneous areas. Another solution is combining several high resolution data as a study by [Zhao et al. \(2019\)](#) that integrated UAV with Sentinel-2A to improve the accuracy of the classification.

CONCLUSION

The NDVI method does not meet the requirements for interpreting land cover classification, because the accuracy was 37.7% in June and 39.9% in October. These results were far from the satellite data processing requirements set by LAPAN, which is 75%. For future work, there is a potential improvement for this method to enhance the vegetation index by using the Normalized Difference Water Index (NDWI) dan Soil Adjusted Vegetation Index (SAVI).

ACKNOWLEDGMENTS

Authors would like to thank the U.S. Geological Survey for Sentinel-2 (ESA) image courtesy.

DECLARATIONS

Conflict of Interest

We declare no conflict of interest, financial or otherwise.

Ethical Approval

On behalf of all authors, the corresponding author states that the paper satisfies Ethical Standards conditions, no human participants, or animals are involved in the research.

Informed Consent

On behalf of all authors, the corresponding author states that no human participants are involved in the research and, therefore, informed consent is not required by them.

DATA AVAILABILITY

Data used to support the findings of this study are available from the corresponding author upon request.

REFERENCES

- Adam, E., Mutanga, O., & Rugege, D. (2010). Multispectral and hyperspectral remote sensing for identification and mapping of wetland vegetation: a review. *Wetlands Ecology and Management*, 18(3), 281–296. <https://doi.org/10.1007/s11273-009-9169-z>
- Ahmed, T., & Singh, D. (2020). Probability density functions based classification of MODIS NDVI time series data and monitoring of vegetation growth cycle. *Advances in Space Research*, 66(4), 873–886. <https://doi.org/10.1016/j.asr.2020.05.004>
- Andiko, J. A., Duryat, & Darmawan, A. (2019). Efisiensi penggunaan citra multisensor untuk pemetaan tutupan lahan. *Jurnal Sylva Lestari*, 7(3), 342–349. <https://doi.org/10.23960/jsl37342-349>
- Arnanto, A. (2013). Pemanfaatan Transformasi Normalized Difference Vegetation Index (NDVI) Citra Landsat TM untuk zonasi vegetasi di lereng merapi bagian selatan. *Geomedia: Majalah Ilmiah Dan Informasi Kegeografian*, 11(2), 155–170. <https://doi.org/10.21831/gm.v11i2.3448>
- Badan Informasi Geospasial. (2017). *Geospasial untuk Negeri. Pusat Pengelolaan Dan Penyebarluasan Informasi Geospasial*. Badan Informasi Geospasial (BIG). Retrieved from <http://tanahair.indonesia.go.id/portal-web>
- Badan Pusat Statistik. (2019). *Kabupaten Jember Dalam Angka 2019*. BPS Kabupaten Jember.
- Bontemps, S., Arias, M., Cara, C., Dedieu, G., Guzzonato, E., Hagolle, O., Inglada, J., Matton, N., Morin, D., Popescu, R., Rabaute, T., Savinaud, M., Sepulcre, G., Valero, S., Ahmad, I., Bégué, A., Wu, B., de Abelleira, D., Diarra, A., ... Defourny, P. (2015). Building a data set over 12 globally distributed sites to support the development of agriculture monitoring applications with Sentinel-2. *Remote Sensing*, 7(12), 16062–16090. <https://doi.org/10.3390/rs71215815>
- Clerici, N., Valbuena Calderón, C. A., & Posada, J. M. (2017). Fusion of sentinel-1a and sentinel-2A data for land cover mapping: A case study in the lower Magdalena region, Colombia. *Journal of Maps*, 13(2), 718–726. <https://doi.org/10.1080/17445647.2017.1372316>

- Cui, L., Li, G., Ren, H., He, L., Liao, H., Ouyang, N., & Zhang, Y. (2014). Assessment of atmospheric correction methods for historical Landsat TM images in the coastal zone: A case study in Jiangsu, China. *European Journal of Remote Sensing*, 47(1), 701–716. <https://doi.org/10.5721/EuJRS20144740>
- da Silva, M. R., de Carvalho, O. A., Guimarães, R. F., Trancoso Gomes, R. A., & Rosa Silva, C. (2020). Wheat planted area detection from the MODIS NDVI time series classification using the nearest neighbour method calculated by the Euclidean distance and cosine similarity measures. *Geocarto International*, 35(13), 1400–1414. <https://doi.org/10.1080/10106049.2019.1581266>
- Dronova, I. (2015). Object-based image analysis in wetland research: A review. *Remote Sensing*, 7(5), 6380–6413. <https://doi.org/10.3390/rs70506380>
- Filgueiras, R., Mantovani, E. C., Althoff, D., Fernandes Filho, E. I., & Cunha, F. F. da. (2019). Crop NDVI monitoring based on sentinel 1. *Remote Sensing*, 11(12), 1441. <https://doi.org/10.3390/rs11121441>
- Firmansyah, S., Gaol, J. L., & Susilo, S. B. (2019). Perbandingan klasifikasi SVM dan Decision Tree untuk pemetaan mangrove berbasis objek menggunakan citra satelit Sentinel-2B di Gili Sulat, Lombok Timur. *Jurnal Pengelolaan Sumberdaya Alam dan Lingkungan (Journal of Natural Resources and Environmental Management)*, 9(3), 746-757. <https://doi.org/10.29244/jpsl.9.3.746-757>
- Goncalves, R. M., Saleem, A., Queiroz, H. A. A., & Awange, J. L. (2019). A fuzzy model integrating shoreline changes, NDVI and settlement influences for coastal zone human impact classification. *Applied Geography*, 113, 102093. <https://doi.org/10.1016/j.apgeog.2019.102093>
- Huang, S., Ming, B., Huang, Q., Leng, G., & Hou, B. (2017). A case study on a combination NDVI forecasting model based on the entropy weight method. *Water Resources Management*, 31(11), 3667–3681. <https://doi.org/10.1007/s11269-017-1692-8>
- Indarto. (2014). *Teori dan Praktik Penginderaan jauh*. Andi Offset.
- Kawamuna, A., Suprayogi, A., & Wijaya, A. P. (2017). Analisis Kesehatan Hutan Mangrove Berdasarkan Metode Klasifikasi NDVI pada Citra Sentinel-2 (Studi Kasus : Teluk Pangpang Kabupaten Banyuwangi). *Geodesi Undip*, 6, 277–284. doi.org/10.14710/jgundip.2017.15439
- Kristianingsih, L., Wijaya, A. P., & Sukmono, A. (2016). Analisis pengaruh koreksi atmosfer terhadap estimasi kandungan klorofil-a menggunakan citra landsat 8. *Jurnal Geodesi Undip*, 5(4), 56–64. <https://doi.org/10.14710/jgundip.2016.13876>
- LAPAN. (2014). *Penyusunan pedoman pengolahan digital klasifikasi penutup lahan menggunakan penginderaan jauh*. Pusat Pemanfaatan Penginderaan Jauh Lembaga Penerbangan dan Antariksa Nasional.

- Menteri Kehutanan Republik Indonesia. (2012). *Peraturan Menteri Kehutanan Republik Indonesia Nomor 32 Tahun 2012 Tentang Tata Cara Penyusunan Rencana Teknik Rehabilitasi Hutan Dan Lahan Daerah Aliran Sungai*. Menteri Kehutanan Republik Indonesia.
- Osgouei, P. E., Kaya, S., Sertel, E., & Alganci, U. (2019). Separating built-up areas from bare land in mediterranean cities using Sentinel-2A imagery. *Remote Sensing*, 11(3). <https://doi.org/10.3390/rs11030345>
- Pandey, P., Dewangan, K. K., & Dewangan, D. K. (2017). Enhancing the quality of satellite images by preprocessing and contrast enhancement. *2017 International Conference on Communication and Signal Processing (ICCSP)*, 56–60.
- Patel, S. K., Verma, P., & Singh, G. S. (2019). Agricultural growth and land use land cover change in peri-urban India. *Environmental Monitoring and Assessment*, 191(9), 1–17. <https://doi.org/10.1007/s10661-019-7736-1>
- Preidl, S., Lange, M., & Doktor, D. (2020). Introducing APiC for regionalised land cover mapping on the national scale using Sentinel-2A imagery. *Remote Sensing of Environment*, 240, 111673. <https://doi.org/10.1016/j.rse.2020.111673>
- Putra, A., Tanto, T. A., Farhan, A. R., Husrin, S., & Pranowo, W. S. (2017). Pendekatan metode Normalized Difference Vegetation Index (NDVI) dan Lyzenga untuk pemetaan sebaran ekosistem perairan di kawasan pesisir teluk Benoa-Bali. *J. Ilmiah Geomatika*, 23(2), 87–94.
- Putra, B. T. W., Soni, P., Marhaenanto, B., Harsono, S. S., & Fountas, S. (2019). Using information from images for plantation monitoring: A review of solutions for smallholders. *Information processing in agriculture*, 7(1), 109-119.. <https://doi.org/10.1016/j.inpa.2019.04.005>
- Saini, R., & Ghosh, S. K. (2021). Crop classification in a heterogeneous agricultural environment using ensemble classifiers and single-date Sentinel-2A imagery. *Geocarto international*, 36(19), 2141-2159. <https://doi.org/10.1080/10106049.2019.1700556>
- Simamora, F. B., Sasmito, B., & Hani'ah. (2015). Kajian metode segmentasi untuk identifikasi tutupan lahan dan luas bidang tanah menggunakan citra pada google earth (Studi Kasus : Kecamatan Tembalang, Semarang). *Jurnal Geodesi Undip*, 4(4), 43–51. <https://doi.org/10.14710/jgundip.2015.9909>
- Sotille, M. E., Bremer, U. F., Vieira, G., Velho, L. F., Petsch, C., & Simões, J. C. (2020). Evaluation of UAV and satellite-derived NDVI to map maritime Antarctic vegetation. *Applied Geography*, 125, 102322. <https://doi.org/10.1016/j.apgeog.2020.102322>
- Sun, R., Chen, S., Su, H., Mi, C., & Jin, N. (2019). The Effect of NDVI time series density derived from spatiotemporal fusion of multisource remote sensing data on crop classification accuracy. *ISPRS International Journal of Geo-Information*, 8(11), 502. <https://doi.org/10.3390/ijgi8110502>
- Tao, H., Li, M., Wang, M., & Lü, G. (2019). Genetic algorithm-based method for forest type classification using multi-temporal NDVI from Landsat TM imagery. *Annals of GIS*, 25(1), 33–43. <https://doi.org/10.1080/19475683.2018.1552621>

- Tsakmakis, I. D., Gikas, G. D., & Sylaios, G. K. (2021). Integration of Sentinel-derived NDVI to reduce uncertainties in the operational field monitoring of maize. *Agricultural Water Management*, 255, 106998. <https://doi.org/10.1016/j.agwat.2021.106998>
- USGS. (2019). EarthExplorer - Home. In U.S. Geological Survey.
- Vali, A., Comai, S., & Matteucci, M. (2020). Deep learning for land use and land cover classification based on hyperspectral and multispectral earth observation data: A review. *Remote Sensing*, 12(15), 2495. <https://doi.org/10.3390/rs12152495>
- Vani, V., & Mandla, V. R. (2017). Comparative Study of NDVI and SAVI vegetation Indices in Anantapur district semi-arid areas. *Int. J. Civ. Eng. Technol*, 8(4).
- Veloso, A., Mermoz, S., Bouvet, A., Le Toan, T., Planells, M., Dejoux, J.-F., & Ceschia, E. (2017). Understanding the temporal behavior of crops using Sentinel-1 and Sentinel-2-like data for agricultural applications. *Remote Sensing of Environment*, 199, 415–426. <https://doi.org/10.1016/j.rse.2017.07.015>
- Vijith, H., & Dodge-Wan, D. (2020). Applicability of MODIS land cover and Enhanced Vegetation Index (EVI) for the assessment of spatial and temporal changes in strength of vegetation in tropical rainforest region of Borneo. *Remote Sensing Applications: Society and Environment*, 18, 100311. <https://doi.org/10.1016/j.rsase.2020.100311>
- Wong, M. M. F., Fung, J. C. H., & Yeung, P. P. S. (2019). High-resolution calculation of the urban vegetation fraction in the Pearl River Delta from the Sentinel-2 NDVI for urban climate model parameterization. *Geoscience Letters*, 6(1), 1–10. <https://doi.org/10.1186/s40562-019-0132-4>
- Yang, Y., Luo, J., Huang, Q., Wu, W., & Sun, Y. (2019). Weighted double-logistic function fitting method for reconstructing the high-quality sentinel-2 NDVI time series data set. *Remote Sensing*, 11(20), 2342. <https://doi.org/10.3390/rs11202342>
- Zhang, H. K., Roy, D. P., Yan, L., Li, Z., Huang, H., Vermote, E., Skakun, S., & Roger, J.-C. (2018). Characterization of Sentinel-2A and Landsat-8 top of atmosphere, surface, and nadir BRDF adjusted reflectance and NDVI differences. *Remote Sensing of Environment*, 215, 482–494. <https://doi.org/10.1016/j.rse.2018.04.031>
- Zhang, T.-X., Su, J.-Y., Liu, C.-J., & Chen, W.-H. (2019). Potential bands of sentinel-2A satellite for classification problems in precision agriculture. *International Journal of Automation and Computing*, 16(1), 16–26. <https://doi.org/10.1007/s11633-018-1143-x>
- Zhao, L., Shi, Y., Liu, B., Hovis, C., Duan, Y., & Shi, Z. (2019). Finer classification of crops by fusing UAV images and Sentinel-2A data. *Remote Sensing*, 11(24), 3012. <https://doi.org/10.3390/rs11243012>